

Cardiac hypertrophy is inhibited by a local pool of cAMP regulated by phosphodiesterase 2

Anna Zoccarato PhD¹, Nicoletta C Surdo PhD², Magnus Aronsen³, PhD, Laura A. Fields PhD¹, Luisa Mancuso PhD⁵, Giuliano Dodoni PhD⁵, Alessandra Stangherlin PhD¹, Craig Livie, PhD¹, He Jiang, MRes¹, Yuan Yan Sin, PhD⁴, Frank Gesellchen, PhD¹, Anna Terrin, PhD¹, George S. Baillie, PhD⁴, Stuart A. Nicklin, PhD⁴, Delyth Graham, PhD⁴, Nicolas Szabo-Fresnaism PhD⁶, Judith Krall, BS⁶, Fabrice Vandeput, PhD⁶, Matthew Movsesian, MD, PhD⁶, Leonardo Furlan, BS⁵, Veronica Corsetti, BS⁵, Graham Hamilton, PhD¹, Konstantinos Lefkimmiatis, PhD², Ivar Sjaastad, MD, PhD³ and Manuela Zaccolo, MD, PhD^{1,2*}

¹Institute of Neuroscience and Psychology and ⁴Institute of Cardiovascular and Medical Sciences, University of Glasgow, Glasgow, UK; ² Department of Physiology, Anatomy and Genetics, University of Oxford, Oxford, UK; ³ Institute for Experimental Medical Research, Oslo University Hospital and University of Oslo, Oslo, Norway, ⁵Venetian Institute of Molecular Medicine, University of Padova, Padova, Italy; ⁶Cardiology Section, VA Salt Lake City Health Care System and Cardiovascular Medicine Division, University of Utah School of Medicine, US.

Short title: PDE2 regulates cardiac hypertrophy

*To whom correspondence should be addressed.

Manuela Zaccolo
Department of Physiology, Anatomy & Genetics,
Sherrington Building,
Parks Road Oxford OX1 3PT, UK.
Tel: ++44 (0)1865 272530
E-mail: manuela.zaccolo@dpag.ox.ac.uk

Word count: 6996

Journal subject code: 15 – Hypertrophy, [107] Biochemistry and metabolism, [138] Cell signalling/signal transduction

Abstract

Rationale: Chronic elevation of 3'-5'-cyclic adenosine monophosphate (cAMP) levels has been associated with cardiac remodelling and cardiac hypertrophy. However, enhancement of particular aspects of cAMP/protein kinase A (PKA) signalling appears to be beneficial for the failing heart. cAMP is a pleiotropic second messenger with the ability to generate multiple functional outcomes in response to different extracellular stimuli with strict fidelity, a feature that relies on the spatial segregation of the cAMP pathway components in signalling microdomains.

Objective: How individual cAMP microdomains impact on cardiac pathophysiology remains largely to be established. The cAMP-degrading enzymes phosphodiesterases (PDEs) play a key role in shaping local changes in cAMP. Here we investigated the effect of specific inhibition of selected PDEs on cardiac myocyte hypertrophic growth.

Methods and results: Using pharmacological and genetic manipulation of PDE activity we found that the rise in cAMP resulting from inhibition of PDE3 and PDE4 induces hypertrophy whereas increasing cAMP levels via PDE2 inhibition is anti-hypertrophic. By real-time imaging of cAMP levels in intact myocytes and selective displacement of PKA isoforms we demonstrate that the anti-hypertrophic effect of PDE2 inhibition involves the generation of a local pool of cAMP and activation of a PKA type II subset leading to phosphorylation of the nuclear factor of activated T cells (NFAT).

Conclusions: Different cAMP pools have opposing effects on cardiac myocyte cell size. PDE2 emerges as a novel key regulator of cardiac hypertrophy both *in vitro* and *in vivo* and its inhibition may have therapeutic applications.

Key words: Hypertrophy, signal transduction, cAMP, protein kinase A, phosphodiesterases 2

1 Non-standard Abbreviations and Acronyms

- 2 AC: adenylyl cyclase
- 3 AKAP: A kinase anchoring protein
- 4 ANP: atrial natriuretic peptide
- 5 ARVM: adult rat ventricular myocyte
- 6 cAMP: 3252cyclic adenosine monophosphate
- 7 CaN: Ca^{2+} -calmodulin dependent phosphatase
- 8 D/D: dimerization/docking domain
- 9 EHNA: (erythro-9-(2-hydroxy-3-nonyl)adenine)
- 10 Epac: Exchange factor activated by cAMP
- 11 FRET: fluorescence resonance energy transfer
- 12 ISO: isoproterenol
- 13 NE: norepinephrine
- 14 NFAT: nuclear factor of activated T cells
- 15 NRVM: neonatal rat ventricular myocyte
- 16 PDE: phosphodiesterase
- 17 PKA: protein kinase A
- 18 PKG: protein kinase G
- 19 TAC: transverse aorta constriction

20

1 Introduction

2 The pleiotropic second messenger 3252cyclic adenosine monophosphate (cAMP) mediates the
 3 catecholaminergic control on heart rate and contractility and, at the same time, is responsible for
 4 the functional response of the heart to a wide variety of other hormones and neurotransmitters.
 5 cAMP signalling is also central to the pathogenesis of a number of conditions including cardiac
 6 hypertrophy, arrhythmia and heart failure¹. An important advance in cardiac adrenergic signal
 7 transduction is the realisation in the past decade that the high fidelity with which cAMP mediates a
 8 plethora of different functions relies on the spatial segregation of the molecular components of this
 9 signalling pathway within subcellular microdomains^{2,3}. The hormonal specificity of cAMP action⁴
 10 results from the generation of distinct pools of the second messenger which in turn mediate
 11 different functional outcomes via activation of different subsets of the cAMP effector protein kinase
 12 A (PKA)^{5,6}. PKA is a holotetrameric enzyme composed of a dimer of regulatory (R) and two
 13 catalytic (C) subunits. In the heart two PKA isoforms are expressed, PKA type I and PKA type II,
 14 which differ in their R subunit. In cardiac myocytes PKA is largely localized to different subcellular
 15 compartments⁶ via binding to a family of scaffolding proteins known as A Kinase Anchoring
 16 Proteins (AKAPs)⁷. Apart from their common ability to anchor PKA, AKAPs show a high degree of
 17 structural variability which allows for different subcellular localisation and binding to a variety of
 18 signalling components. As a result, AKAPs serve as signalling centres, where specific binding
 19 partners are organised for a particular task. Localisation of PKA is achieved through the interaction
 20 of the amino-terminal dimerization/docking (DD) domain of the R subunits⁸ with the AKAP, and
 21 serves to anchor PKA in proximity to selected targets thus favouring their preferential
 22 phosphorylation⁹⁻¹¹. The AKAP-DD interaction is also responsible for differential targeting of the
 23 two PKA isoforms, with different AKAPs showing different specificity of binding for RI and RII¹² as
 24 a consequence of differences within the docking interface in R¹³.

25 The intracellular concentration of cAMP is tightly regulated by the cyclic nucleotide degrading
 26 enzymes PDEs. PDEs are a large superfamily of enzymes including 11 families (PDE1-11) with a
 27 number of different genes and splice variants generating close to 100 isozymes showing unique
 28 kinetic, regulatory and subcellular localization properties¹⁴. PDEs play a pivotal role in shaping
 29 local cAMP signals by limiting cAMP diffusion beyond a microdomain and by regulating cAMP
 30 levels within a microdomain. As a consequence, inhibition of individual PDE families results in a
 31 compartmentalised increase in cAMP as shown by studies using targeted reporters and real time
 32 imaging of cAMP levels in intact myocytes^{15,16}.

33 We have previously reported that in intact neonatal rat ventricular myocytes (NRVMs) PDE2, PDE3
 34 and PDE4 are localised at distinct subcellular sites and uniquely modulate the cAMP response to
 35 individual extracellular stimuli^{17,18}. In NRVM cell lysates PDE3 and PDE4 account for most of the
 36 PDE activity whereas PDE2 is responsible for only a minor fraction of cAMP hydrolytic activity¹⁷.
 37 However, in intact NRVMs, in spite of its low abundance, PDE2 plays a major role in the control of
 38 the cAMP response to catecholamines¹⁸, an effect that relies on its specific localisation within the
 39 cell¹⁶.

40
 41 Although the concept of compartmentalised cAMP/PKA signalling in cardiac myocytes is well
 42 established and the physiological function downstream of individual cAMP pools is being
 43 elucidated^{10,11,19,20}, very little is known about the role of local cAMP pools in the pathogenesis of
 44 heart disease. Catecholamines induce cardiac hypertrophy via mechanisms that include activation
 45 of β -adrenergic receptors, generation of cAMP and PKA-mediated elevation of intracellular Ca^{2+} ²¹.
 46 Although chronic stimulation of β -adrenergic signalling leads to pathologic sequelae, enhancement
 47 of particular aspects of cAMP/PKA signalling benefits the failing heart²²⁻²⁴, suggesting that different
 48 components of this pathway may have different consequences on cardiac hypertrophy and failure.

49
 50 In this study we investigate the effect on cardiac hypertrophy of local manipulation of cAMP levels
 51 via selective inhibition of individual PDEs. We find that distinct pools of cAMP differently affect
 52 cardiac myocyte hypertrophic growth and that inhibition of PDE2, unlike inhibition of PDE3 or
 53 PDE4, results in anti-hypertrophic effects both *in vitro* and *in vivo*. We further demonstrate that

increased PDE2 activity is sufficient *per se* to induce hypertrophy. The anti-hypertrophic effect of PDE2 inhibition relies on a local increase in cAMP that enhances PKA-mediated phosphorylation of NFAT and its consequent retention in the cytosol. We conclude that PDE2 regulates a pool of cAMP with unique effects on cardiac myocyte hypertrophic growth and identify PDE2 as a potential novel therapeutic target.

Materials and Methods

A detailed description of the Materials and Methods is included in the online data supplement to this article.

Results

PDE2 inhibition counteracts cardiac myocyte hypertrophy both *in vitro* and *in vivo*.

Treatment of NRVMs with 10 $\mu\text{mol/L}$ norepinephrine (NE) for 48 hours is a well-established *in vitro* model of cardiac hypertrophy²⁵ eliciting the expected hypertrophy markers, including increase in cell surface area, ³H-leucine incorporation, nuclear translocation of NFAT (**Fig. 1B-D**) and ANP levels (**Suppl. Fig. 1A**). To investigate the effect of raising cAMP levels on cardiac myocyte hypertrophy, we treated NRVMs with different cAMP-raising agents (**Fig. 1A**). Activation of adenylyl cyclase with 1 $\mu\text{mol/L}$ forskolin, inhibition of PDE4 with 10 $\mu\text{mol/L}$ rolipram and inhibition of PDE3 with 10 $\mu\text{mol/L}$ cilostamide generated significant hypertrophy (**Fig. 1B-D**). In contrast, inhibition of PDE2 with BAY 60-7550 (10 $\mu\text{mol/L}$) did not induce hypertrophy (**Fig. 1B-D**), despite generating an increase in cAMP as the other treatments (**Fig. 1A**). The unique effect of PDE2 inhibition was also apparent in cells co-treated with NE. When cilostamide and rolipram were administered in combination with 10 $\mu\text{mol/L}$ NE, NE further increased cell size compared to inhibitor alone, although no further enhancement of hypertrophy was observed compared to NE alone (compare **Fig. 1B-D** and **1F-I**). In contrast, BAY 60-7550 blocked the hypertrophic growth induced by NE (**Fig. 1 F-I** and **Suppl Fig 1A-F**), despite its potentiation of the NE-induced cAMP response (**Fig. 1E**). The anti-hypertrophic effect of BAY 60-7550 was confirmed at 50 nmol/L of inhibitor (**Suppl. Fig. 1B**). Similar results were found with EHNA (erythro-9-(2-hydroxy-3-nonyl)adenine), another selective PDE2 inhibitor (**Suppl. Fig. 1C**), in cardiomyocytes from neonatal mice (**Suppl. Fig. 1D**) and in adult rat ventricular myocytes (ARVMs) (**Suppl. Fig. 1E-F**). Similar effects on cell size (**Fig. 1J**) and NFAT-GFP nuclear translocation (**Fig. 1K**) were found when PDE2 expression was knocked down using the small interfering RNA sequence siPDE2¹⁶. The specificity of the siRNA effect was confirmed by rescue experiments (**Suppl. Fig. 2**). BAY 60-7550 also blocked the hypertrophy induced by treatment with 10 $\mu\text{mol/L}$ isoproterenol (**Fig. 1G**) whereas it had no effect on the hypertrophy induced by phenylephrine (PE, **Fig. 1L**), indicating that PDE2 acts downstream of the β - rather than the α -adrenergic receptor. Consistently, Bay 60-7550 did not inhibit PE-induced NFAT nuclear translocation (**Suppl. Fig. 1G**) and did not affect the nuclear translocation of NFAT in response to PE and selective inhibition of GSK3 β and JNK (**Suppl. Fig. 1G**), indicating that inhibition of PDE2 acts independently of this pathway. To examine whether PDE2 inhibition also attenuates cardiac hypertrophy *in vivo*, adult C57Bl/6 mice were subjected to transverse aorta constriction (TAC) for 3 weeks and concurrently treated with BAY 60-7550 (3mg/kg) or with vehicle (**Suppl. Table 1**). The PDE2 inhibitor induced a significant reduction of cardiac hypertrophy as verified by echocardiography (**Suppl. Fig. 1H-I**), cardiac MRI (**Fig. 2 A-B**) and post-mortem examination (**Fig. 2C-H**).

PDE2 overexpression results in cardiac myocyte hypertrophy both *in vitro* and *in vivo*. We next investigated the effect of increasing PDE2 activity in NRVMs by overexpressing a Red Fluorescent Protein-tagged version of PDE2 (PDE2Awt-mRFP). We found a significant increase in cell surface area (**Fig. 3A-B**) and in nuclear translocation of NFAT-GFP (**Fig. 3C**) in transfected versus untransfected cells. Overexpression of a catalytically inactive version of the enzyme (dnPDE2Awt-mRFP) had no effect (**Fig 3D and 5E**). Similar results were found in ARVMs (**Suppl. Fig. 3A-D**). To test whether overexpression of PDE2 results in hypertrophic growth *in vivo*, a recombinant adenoviral vector (Ad) expressing the PDE2A enzyme tagged with mCherry

(AdV5/PDE2Awt-mCherry) was injected in the heart of adult rats. Seven days after injection, the cell surface areas of transduced and untransduced myocytes dissociated from the same heart were compared. As shown in **Fig. 3E-F**, PDE2Awt-mCherry expressing cardiomyocytes show a significant increase in cell surface area as compared to untransduced cells; cardiomyocytes overexpressing the catalytically inactive PDE2Adn-mCherry did not differ from untransduced cells (**Fig. 3E, G**).

The anti-hypertrophic effect of PDE2 inhibition is PKA-dependent. PDE2 can degrade both cAMP and cGMP²⁶ therefore its inhibition may result in an increase of both second messengers. To establish whether PKA or PKG mediates the anti-hypertrophic effect of PDE2 inhibition we measured cell surface area and NFAT-GFP nuclear translocation in NE-treated NRVMs in the presence of selective kinase inhibitors. The selective PKG inhibitor DT-2²⁷ did not affect the ability of BAY 60-7550 to significantly reduce hypertrophy (**Fig. 4A, B**). As a control we measured the effect of DT-2 on the anti-hypertrophic effect of selective inhibition of the cGMP-specific PDE5 with sildenafil (10 nmol/L), previously reported to counteract hypertrophy via PKG activity²⁸. We found that sildenafil alone had no effect on either cells surface area or NFAT-GFP nuclear translocation (**Suppl. Fig. 4**) but DT-2 completely blocked the cGMP-mediated effect of sildenafil on NE-induced cell size increase (**Fig. 4A**) and NFAT-GFP nuclear translocation (**Fig. 4B**). In contrast, selective PKA inhibition with myrPKI²⁹ completely abolished the anti-hypertrophic effects of BAY 60-7550 (**Fig. 4C,D**) without affecting the anti-hypertrophic effect of sildenafil (**Fig. 4C-D**). In keeping with these findings, the effect of PDE2 knock-down on NE-induced hypertrophy was completely blocked by myrPKI but was unaffected by DT-2 treatment (**Fig. 4E-F**). Consistent with a role for PKA activation downstream of PDE2 inhibition, we found that Bay 60-7550 significantly increases PKA-mediated phosphorylation of the FRET reporter AKAR4 (**Suppl. Fig. 5**). The role of PKA is further supported by the finding that the anti-hypertrophic effect of BAY 60-7550 is completely blocked by the PKA inhibitors H89 and cAMPS-Rp (**Fig. 4G**). In addition, we found that disrupting PKA-AKAPs interactions with the competing peptide Ht31³⁰ abolishes the effect of BAY 60-7550 on nuclear translocation of NFAT, (**Fig. 4H**), confirming a PKA-dependent mechanism and indicating that a localised subset of PKA is involved. Thus, the anti-hypertrophic effect of PDE2 is PKA-mediated and PKG-independent.

PDE2 modulates a local pool of cAMP with anti-hypertrophic effects. PDE2 has been shown to be targeted to specific subcellular sites in NRVMs¹⁸, a finding that we confirm here in ARVMs (**Suppl. Fig. 6**). A possible explanation for the opposite effect on cell size observed on selective PDE inhibition is that blocking the activity of a localised PDE2 raises cAMP content in a specific subcellular microdomain that is linked to anti-hypertrophic effects, whereas inhibition of PDE3 and PDE4 increases cAMP at sites where pro-hypertrophic effectors are activated. If so, it should be possible to recapitulate the effect of selective pharmacological inhibition by displacing the individual PDEs from their anchor sites within the cell, a manoeuvre that has been previously used to generate a localised increase in cAMP^{16, 31}. To test this, we measured cell surface area in NRVMs overexpressing fluorescent protein-tagged chimeras of catalytically inactive mutants of PDE2A (PDE2Adn)¹⁶, PDE3A2 (PDE3A2dn) and PDE4D3 (PDE4D3dn)³². We found that displacement of endogenous PDE4D3 (**Fig. 5A**) or PDE3A2 (**Fig. 5C**) resulted in hypertrophy, and did not further increase the hypertrophy induced by NE treatment (**Fig. 5B, D**), reproducing the effects of pharmacological inhibition. In contrast, displacement of endogenous PDE2A did not affect cell size in untreated myocytes (**Fig. 5E**) but significantly reduced the hypertrophy induced by NE (**Fig. 5F**). Similar results were found for nuclear translocation of NFAT-GFP (**Suppl. Fig. 7A, B**) and in ARVMs (**Suppl. Fig. 7C-F**). These data support a model whereby different PDEs localised to different intracellular locations control distinct pools of cAMP with opposite effects on cardiac myocyte cell size.

The anti-hypertrophic effect of PDE2 inhibition is mediated by PKAII. The data presented so far demonstrate that a local pool of cAMP with anti-hypertrophic effects is selectively regulated by PDE2-mediated hydrolysis. To gain some insight into the subcellular localisation of such a pool we

measured the cAMP signal generated on selective PDE2 inhibition using RI_epac and RII_epac, two FRET-based reporters for cAMP that localise to the sites where PKAI and PKAII, respectively, normally reside within the cell. These reporters target to different AKAPs and have been previously shown to selectively detect cAMP signals within distinct subcellular compartments⁶. PDE2 inhibition potentiates the cAMP response to 10 nmol/l NE (**Fig. 6A**) or 10 nmol/L ISO (**Suppl. Fig. 8A**) both in the PKAI and PKAII compartments, whereas PDE3 inhibition affects the cAMP response exclusively in the PKAI compartment (**Fig. 6B and Suppl. Fig. 8B**). Similar results were found in ARVM (**Suppl. Fig 8D-E**). As inhibition of PDE3 promotes, rather than inhibit, hypertrophy (**Fig 1A, D**) we hypothesised that the cAMP pool under the control of PDE2 and responsible for the anti-hypertrophic effect is associated with the PKAII compartment. Consistent with this model we found that, on inhibition of PDE2, PKA-mediated phosphorylation is significantly higher in the PKAII compartment as opposed to the PKAI compartment (**Fig 6D**). In addition, the effect of PDE2 inhibition on hypertrophy was completely blocked by SuperAKAP-IS¹², a peptide that disrupts selectively the interaction between PKAII and AKAPs, whereas the PKAI-AKAP selective disruptor RIAD³³ had no effect (**Fig 6E-F**), confirming that a subset of AKAP-anchored PKAII mediates the antihypertrophic effect downstream of PDE2 inhibition. Interestingly, the pro-hypertrophic effect of PDE3 and PDE4 inhibition, although PKA-dependent (**Fig 6G**) was not affected by treatment with either SuperAKAP-IS or RIAD (**Fig 6H-I**), suggesting that the prohypertrophic effect of PDE3 and PDE4 inhibition does not require an AKAP-anchored subset of PKA.

The anti-hypertrophic effect of PDE2 inhibition requires PKA-mediated phosphorylation of NFAT. Nuclear translocation of NFAT regulates pathological cardiac hypertrophy³⁴. PKA phosphorylates NFAT at Ser 245, Ser 269 and Ser 294³⁵, thus preventing its nuclear translocation³⁶. We therefore hypothesised that the anti-hypertrophic effects of PDE2 inhibition may rely on PKA-mediated phosphorylation of NFAT. Consistent with our hypothesis treatment of NRVM with Bay 60-7550 results in strong enhancement of PKA-dependent phosphorylation of NFAT (**Fig 7A**). In addition, in a pull-down of PKA-phosphorylated proteins from lysates of NRVMs hypertrophied *in vitro* the amount of PKA-phosphorylated NFAT-GFP was significantly higher in BAY 60-7550 treated than in control cells (**Fig. 7B and Suppl. Fig. 9C-D**). Similar results were obtained from NFAT-GFP pull downs probed with a PKA substrate antibody (**Suppl Fig. 9A-B**). Notably, increased phosphorylation on inhibition of PDE2 was confirmed when probing for endogenous NFAT (**Fig. 7 C**). It is interesting to note that PDE4 inhibition increase PKA-mediated phosphorylation of overexpressed NFAT-GFP (**Fig. 7B and Suppl. Fig. 9C-D**), in line with the large global rise in cAMP that it generates (**Fig. 1C**). Overexpressed NFAT is likely to distribute to sites where endogenous NFAT normally is not present and therefore it is expected to become phosphorylated on PDE4 inhibition. However, PDE4 inhibition does not significantly affect the phosphorylation of endogenous NFAT (**Fig. 7C**), further confirming that PDE2 and PDE4 act on distinct pools of cAMP and have distinct effects on the endogenous protein. To further test whether the anti-hypertrophic effect of BAY 65-7550 is mediated by PKA-dependent phosphorylation of NFAT, we generated a PKA phosphorylation-resistant form of NFAT-GFP by introducing serine-to-alanine substitutions at positions 245, 269 and 294. BAY 60-7550 reduced the translocation of wild type NFAT-GFP but did not affect nuclear translocation of triple-mutant NFAT-GFP (**Fig. 7D**), indicating that the PKA-phosphorylation sites on NFAT are required for BAY 60-7550 to prevent NE-induced nuclear translocation of NFAT. In contrast, treatment of hypertrophic myocytes with sildenafil significantly blocked nuclear translocation of both wild type and triple mutant NFAT-GFP (**Fig. 7D**), as expected given that the anti-hypertrophic effect mediated by sildenafil is independent of PKA phosphorylation (**Fig. 2 and 27**). Inhibition of PDE4 with rolipram did not affect the nuclear translocation of either wt or triple-mutant NFAT (**Fig. 7D**). In further support of the role of a local pool of cAMP in the anti-hypertrophic effect of PDE2 inhibition, overexpression of PDE2Adn-mRFP in NE-treated NRVMs reduced nuclear translocation of NFAT-GFP (**Suppl. Fig. 10A**) but not of triple mutant NFAT-GFP (**Suppl. Fig. 10B**). In addition, in the presence of triple mutant NFAT-GFP, PDE2Adn-mRFP was unable to counteract NE-induced hypertrophy (**Suppl. Fig. 10C-D**), further confirming that the anti-hypertrophic effect of PDE2 requires PKA-mediated phosphorylation of NFAT. The involvement of NFAT phosphorylation and NFAT-dependent gene transcription in the anti-hypertrophic effect of PDE2 inhibition *in vivo* was confirmed in experiments where we

measured NFAT phosphorylation (**Fig. 7E**) and mRNA levels for BNP and RCAN1 (**Fig. 7F**), two genes that are transcribed under the control of NFAT^{34, 37} in sham operated, TAC+vehicle and TAC+BAY 60-7550 treated mice. We found that treatment with the PDE2 inhibitor significantly enhances NFAT phosphorylation and reduces the level of expression of NFAT-dependent genes, thus reversing the molecular fingerprint of pathological hypertrophy. To further support our conclusion that PDE2 inhibition counteracts cardiac hypertrophy *in vivo* via an NFAT-dependent mechanism we subjected NFAT reporter mice³⁸ to TAC and randomization to treatment with BAY 60-7550 or vehicle for two weeks (**Suppl. Table 2 and Suppl. Figure 11**). In line with our previous results BAY 60-7550 treated NFAT reporter mice showed reduced cardiac hypertrophy (**Suppl. Fig 11**) and corresponding NFAT luciferase activity (**Fig. 7G**) after TAC as compared to vehicle treated mice.

Discussion

In this study we identify PDE2 as a regulator of cardiac hypertrophy by providing strong evidence, both *in vitro* and *in vivo*, that overexpression of PDE2 is sufficient *per se* to induce hypertrophy and that inhibition of PDE2 counteracts cardiac myocyte hypertrophic growth, an effect that relies on cAMP-dependent activation of PKA. Our data reveal a completely novel mechanism through which cAMP signalling impacts cardiac myocyte cell size that strictly depends on the subcellular site at which the cAMP signal is generated. Thus, inhibition of PDE2 generates a local pool of cAMP with anti-hypertrophic effects, whereas the rise in cAMP generated via inhibition of PDE3 or PDE4 has pro-hypertrophic effects. We demonstrate here for the first time that spatially distinct pools of cAMP can be generated downstream of β AR activation with opposing effects on myocyte cell size.

Using targeted FRET reporters for cAMP and selective displacement of PKAI and PKAII from their anchoring sites on AKAPs we unveil a complex involvement of cAMP and PKA in regulation of cardiac myocyte hypertrophic growth. Inhibition of PDE2 and PDE4 results in a cAMP increase in both the PKAI and PKAII compartments, yet the effect on cell size is opposite. To rationalise these findings, it should be noted that in cardiac myocytes there are multiple PKAI-AKAP and PKAII-AKAP complexes⁷ and that the PKAI- and PKAII-targeted FRET reporters do not discriminate between individual complexes. Thus, although inhibition of both PDE2 and PDE4 generates a predominant rise in cAMP in the PKAII compartment, the rise in cAMP may affect different PKAII-AKAP complexes. Our findings support a model whereby a pool of cAMP generated in the PKAII compartment on PDE2 inhibition counteracts hypertrophy whereas a pool of cAMP generated on inhibition of PDE4 within the PKAII compartment, but presumably involving different PKAII-AKAP complexes, has no effect on cell size. Alternatively, inhibition of PDE4 may affect the same pool of cAMP under the control of PDE2, but a concomitant increase in cAMP at a different site has a dominant, pro-hypertrophic effect. In support of the latter, using PKA-AKAP selective disruptors we find that inhibition of PDE4, as well as inhibition of PDE3, result in hypertrophy via activation of a subset of PKA that is not anchored to AKAPs.

It is well established that adrenergic stimulation can initiate cardiac hypertrophy via generation of cAMP and activation of PKA^{39, 40}, as confirmed by PKA knockout studies in which deletion of PKA subunits is protective against hypertrophy⁴¹. Other studies, however, have suggested that components of the β -adrenergic signalling pathway may play a protective role in response to haemodynamic overload. For example, it has been reported that over-expression of some types of adenylyl cyclase improve cardiac function²³ and that PKA-mediated phosphorylation of histone deacetylase 5 prevents its nuclear export and results in decreased cardiac myocyte size⁴². The present data support the coexistence within the same cell of multiple spatially segregated cAMP/PKA signalling pathways that can alternatively prevail depending on the status of the cell and provide a possible mechanistic basis for the dichotomy reported in the literature on the role of PKA on the development of cardiac pathology.

Dephosphorylation of NFAT and its subsequent translocation to the nucleus is regulated by the Ca^{2+} -calmodulin dependent phosphatase (CaN), one of the most potent activators of the

hypertrophic programme³⁴. It is interesting to note that CaN can directly interact with a number of AKAPs, including AKAP1⁴³, AKAP5⁴⁴ and AKAP6⁴⁵, all of which bind PKA type II. In addition, studies suggest that regulation of CaN activity occurs via a specific microdomain of Ca²⁺⁴⁶, further supporting a local regulation of this phosphatase. Although NFAT has not been reported to be part of a macromolecular complex organised by AKAPs, there is some evidence that this transcription factor also resides in distinct cytosolic domains and that its regulation occurs locally⁴⁷. Based on the above observations, a possible scenario is therefore that PDE2 controls a pool of cAMP that activates an AKAP-bound PKA type II to phosphorylate a local NFAT, possibly counterbalancing its dephosphorylation by a local CaN. Further studies are required to explore this hypothesis.

Recently it has been reported by Mehel et al. that NE treatment does not significantly increase cell size in ARVM overexpressing PDE2⁴⁸. Based on this observation the authors suggest that PDE2 may be protective against pathological hypertrophy. Unfortunately that report show only normalised values of the effect of NE on cells overexpressing PDE2 and not the effect on cell size of overexpression of PDE2 *per se*, making the data difficult to interpret. We note however that, although the authors draw to the opposite conclusion, the data as reported by Mehel et al. are compatible with the findings described in the present report. If we were to express the effect of NE on cell size relative to control cells and relative to PDE2 overexpressing cells, as reported in the Mehel et al study, the latter group would show a significantly blunted effect of NE treatment (see **Suppl. Fig. 12** and refer to **Suppl. Fig. 3A-B** and **Suppl. Fig. 7E-F**). However, this way of presenting the data is misleading as overexpression of PDE2 already results in very significant hypertrophy compared to control cells (see **Fig. 3** and **Suppl. Fig. 3**), thus reducing the relative effect of NE.

Our findings may have important clinical implications. The *in vivo* data provide a first indication that inhibition of PDE2 counteracts hypertrophy in a TAC model. Additional investigations will be required to establish whether this would protect from progression toward heart failure and the relevance of PDE2 activity to human cardiac hypertrophy. Interestingly, increased levels of PDE2 expression have been reported in early rat cardiac hypertrophy⁴⁹ as well as in failing human hearts⁵⁰, suggesting that increased activity of this enzyme may be involved in the pathogenesis of the disease. It has been suggested that the hypertrophic response to pathological stress is never truly 'adaptive'⁵¹ and that inhibition of hypertrophy is beneficial⁵²⁻⁵⁴. In addition the possibility to control the local concentration of cAMP at specific sites via selective inhibition of PDEs has been previously recognized as a possible approach to improving clinical outcomes⁵⁵ and a phase 3 trial has been recently concluded where the PDE3 selective inhibitor enoximone was used in combination with β -blockade to couple inhibition of adverse β -adrenergic signalling with restoration of phospholamban phosphorylation⁵⁶. In this perspective, PDE2 may represent a particularly interesting target. *In vitro* studies have demonstrated that the pool of cAMP generated upon inhibition of PDE2 mediates positive inotropic effects^{18, 57} and the ability to manipulate a pool of cAMP that simultaneously exerts positive inotropy and counteracts cardiac myocyte hypertrophic growth may represent a significant improvement over existing therapeutic strategies.

Source of Funding

This study was supported by the Fondation Leducq (O6 CVD 02), the British Heart Foundation (PG/10/75/28537 and RG/12/3/29423) to MZ.

Disclosures: None

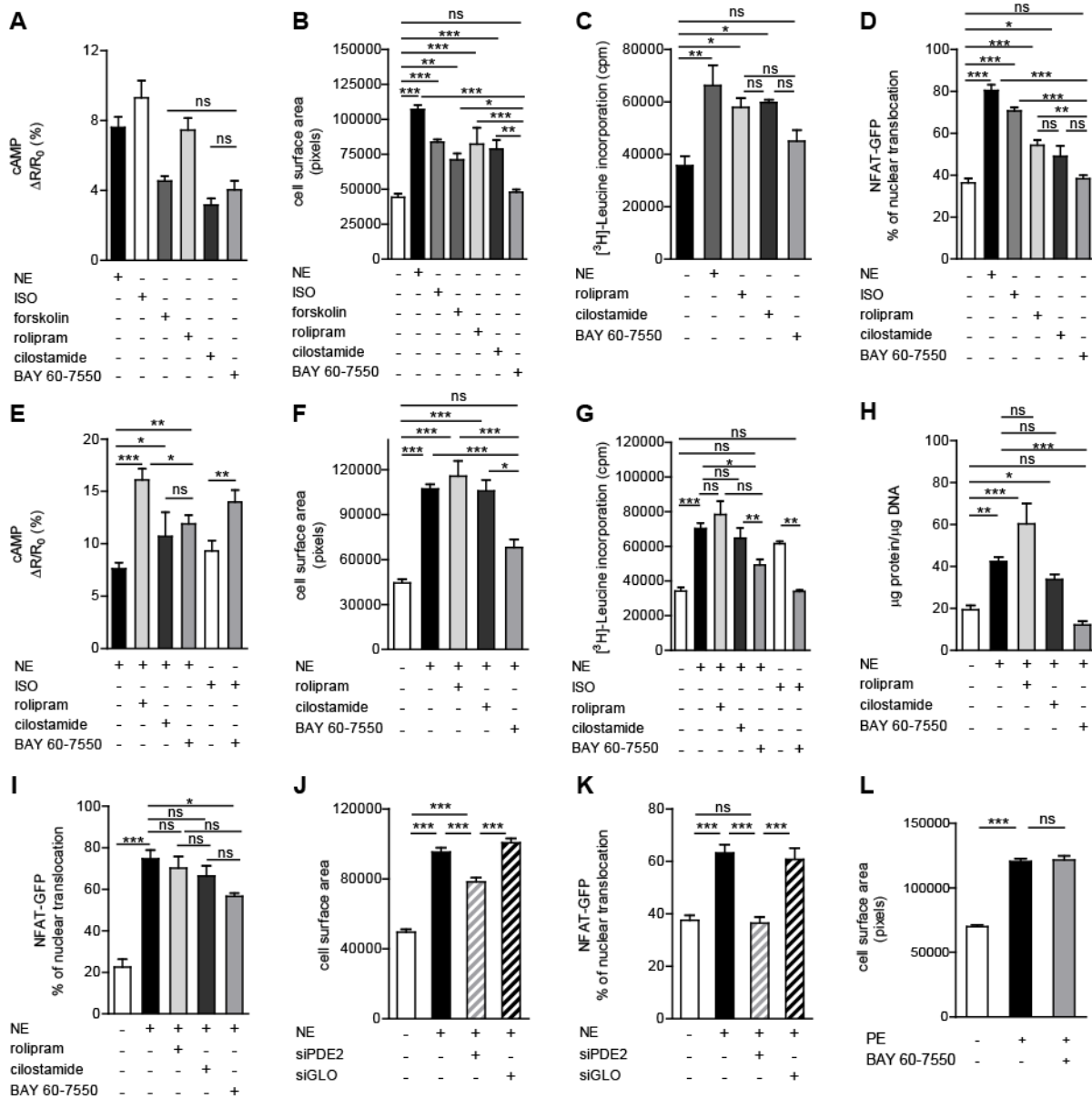


Figure 1. Effect of PDE2 inhibition on cardiac myocyte hypertrophy *in vitro*

(A) cAMP increase induced by 1nmol/L NE, 10nmol/L ISO, 1 μ mol/L forskolin, 10 μ mol/L rolipram, 10 μ mol/L cilostamide or 10 μ mol/L BAY 60-7550 measured in NRVMs using real-time FRET imaging (ne4 cells). (B) Cell surface area of NRVMs treated for 48 hours with NE (10 μ mol/L), ISO (10 μ mol/L), forskolin (1 μ mol/L), rolipram (10 μ mol/L), cilostamide (10 μ mol/L), and BAY 60-7550 (10 μ mol/L) or untreated control. ne32 cells. (C) [3 H] leucine incorporation (n e 16 independent experiments) and (D) NFAT-GFP nuclear translocation measurements (minimum of 3 independent experiments) calculated for untreated NRVMs, or NRVMs treated as indicated. (E) FRET measurements of cAMP levels in NRVMs upon stimulation with NE (1 nmol/L), and NE in combination with 10 μ mol/L rolipram, 10 μ mol/L cilostamide or 10 μ mol/L BAY 60-7550. (F) Cell surface area (ne44 cells), (G) [3 H] leucine incorporation (n e 27 independent experiments), (H) normalised protein content and (I) NFAT-GFP nuclear translocation measured in NRVMs untreated or treated for 48 hours as indicated. (J) Cell surface area (minimum of n=128 cells per condition) and (K) NFAT-GFP nuclear translocation (minimum of 5 independent experiments) for control, NE (10 μ mol/L)-treated NRVMs and NRVMs treated with NE (10 μ mol/L) and transfected either with siPDE2 or with the control oligo siGLO Red. (L) Cell surface area of NRVMs treated for 48 hours

1 as indicated; PE (1 $\mu\text{mol/L}$), BAY 60-7550 (10 $\mu\text{mol/L}$); ne135 cells. All data represent mean \pm
2 s.e.m. One-way ANOVA and Tukey's multiple comparison tests were performed. Pixel size =
3 0.1075 μm . * $p < 0.05$; ** $p < 0.01$; *** $p < 0.005$; ns = not significant.

4

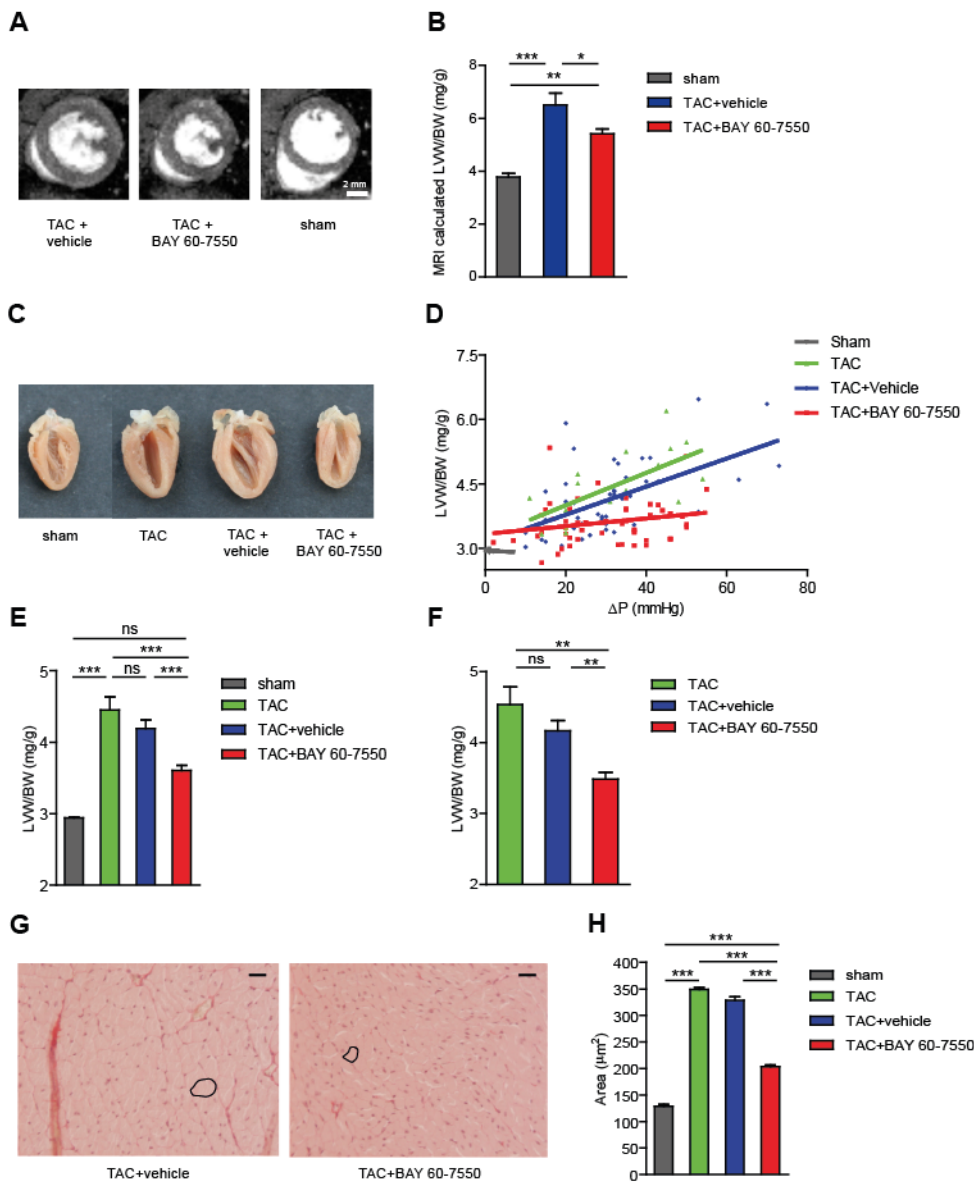


Figure 2. PDE2 inhibition attenuates cardiac hypertrophy *in vivo*.

(A) Representative mid ventricular MRI short axis images of left ventricle in end diastole treated for 3 weeks as indicated. (B) Left ventricular weight calculated from MRI recordings divided by body weight as indicated. (C) Representative heart sections obtained from mouse hearts extracted 3 weeks after sham or TAC operation in the absence or presence of treatment, as indicated. (D) Left ventricular weight, body weight ratio (LVW/BW) plotted against the systolic pressure gradient calculated as a difference between right and left carotid systolic blood pressure (ΔP) at 3 weeks after sham operation, TAC, TAC+vehicle or TAC+BAY 60-7550 (3 mg/kg). (E) Summary and comparison of mean LVW/BW ratio values calculated for all sham-operated, TAC, TAC+vehicle or TAC+BAY 60-7550 treated mice. (F) Mean LVW/BW ratio values calculated for TAC, TAC+vehicle or TAC+BAY 60-7550 treated mice presenting with a ΔP within the 30-40mmHg range. (G) Representative images of picrosirius red staining of heart sections generated after 3 weeks of TAC and treatment with vehicle or BAY 60-7550. In each panel, the contour of a representative cell is highlighted with a black line. Scale bar = 40 μm . (H) Summary of myocyte cross-sectional area from sham, TAC, TAC+vehicle and TAC+BAY 60-7550 treated hearts (mean \pm s.e.m of at least n=213).

1 cells per condition). One-way ANOVA and Tukey's multiple comparison tests were performed in all
2 experiments. *pd0.05; **pd0.01; ***pd0.005.

3

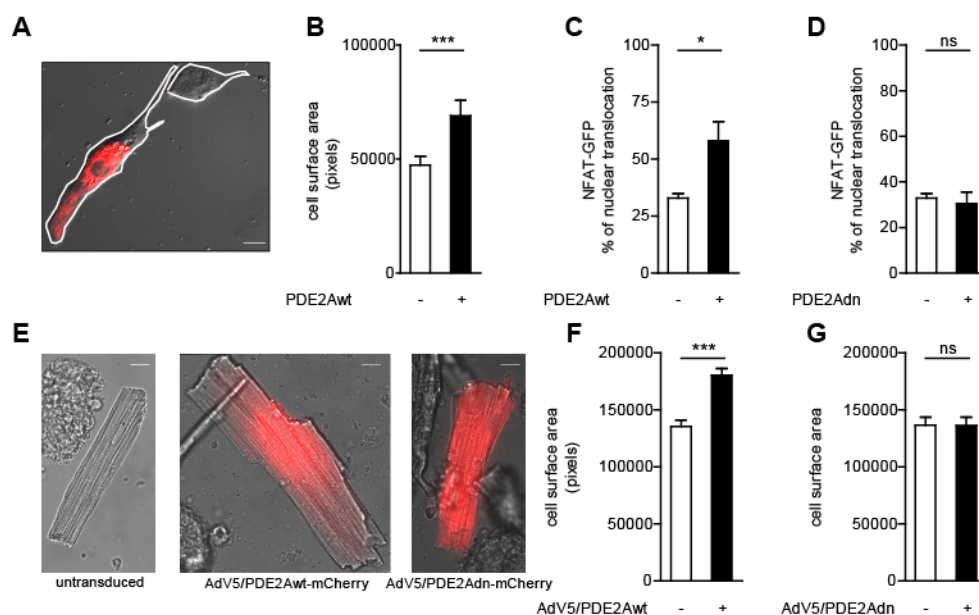


Figure 3. PDE2 overexpression induces cardiac myocyte hypertrophic growth *in vitro* and *in vivo*.

(A) Overlay of differential interference contrast (DIC) and fluorescence images showing in the same field one NRVM overexpressing PDE2Awt-mRFP and one untransfected control cardiomyocyte. Cell contour is highlighted in white (Scale bar: 10 μ m). **(B)** Cell surface area (3 independent experiments, ne49) calculated for untransfected NRVMs or NRVMs overexpressing PDE2Awt-mRFP (Pixel size = 0.1075 μ m). **(C-D)** Percentage of cells showing nuclear translocation of NFAT-GFP measured for untransfected control NRVMs, NRVMs overexpressing PDE2Awt-mRFP or PDE2A2dn-mRFP (4 independent experiments, total cell number e47). **(E)** Representative images of a untransduced (left panel) and transduced ARVMs expressing AdV5/PDE2Awt-mCherry (middle panel) or the catalytically inactive AdV5/PDE2Adn-mCherry (right panel). **(F)** Summary of cell surface area of ARVMs transduced with AdV5/PDE2wt-mCherry and untransduced myocytes isolated from the same heart. **(G)** Cell surface area of ARVMs obtained from hearts injected with AdV5/PDE2Adn-mCherry and expressing or not expressing the catalytically inactive recombinant enzyme. Consistent results were obtained from hearts from 3 different animals injected with AdV5/PDE2Awt-mcherry and 3 animals injected with AdV5/PDE2Adn-mcherry; number of cells for each condition e100. Pixel size = 0.1613 μ m. All data represent mean \pm s.e.m. For all experiments *t*-test statistical analysis was performed. * *p* < 0.05, *** *p* < 0.005.

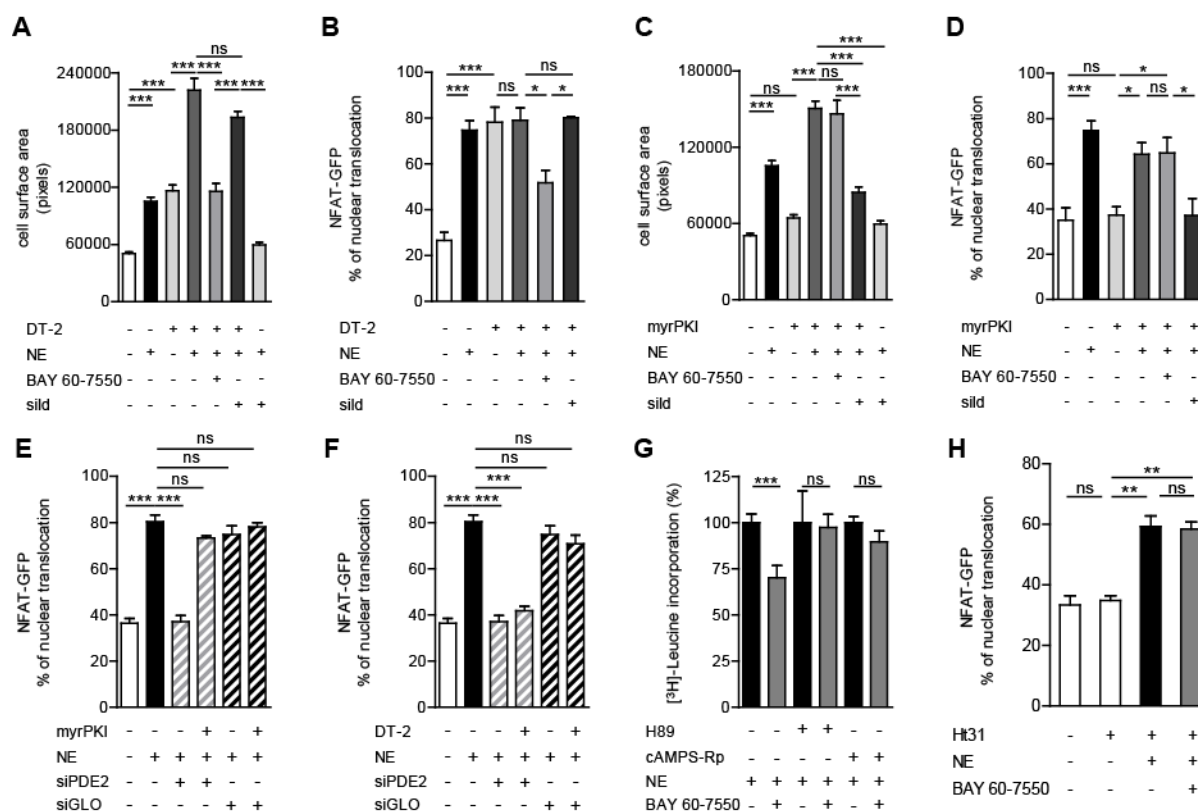
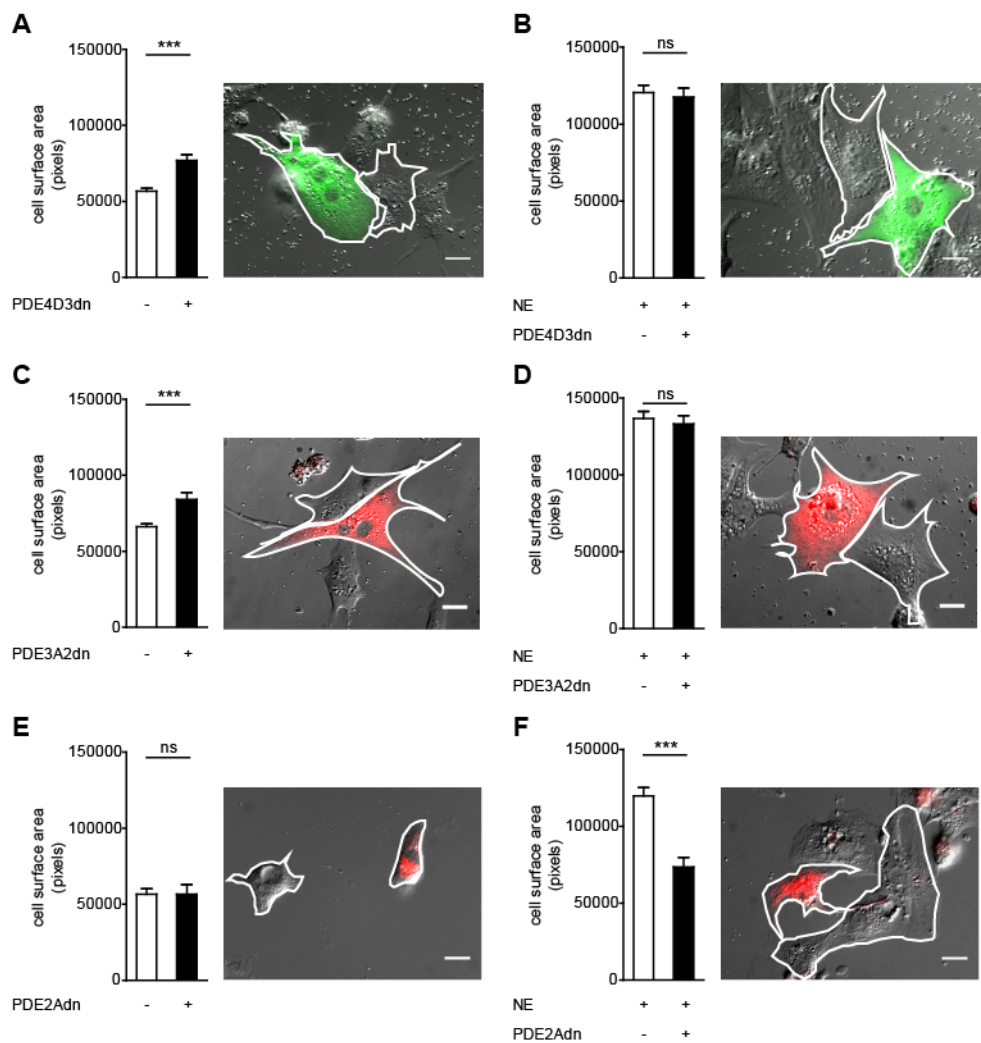


Figure 4. The anti-hypertrophic effect of PDE2 inhibition is PKA-dependent.

(A) Cell surface area (3 independent experiments, ne72) and **(B)** NFAT-GFP nuclear translocation (3 independent experiments, n e50) measurements for untreated control, NRVMs treated for 48 hours with NE (10 μ mol/L) or DT-2 (10 μ mol/L), or treated with DT-2 in combination with NE, NE and BAY 60-7550 (10 μ mol/L), or NE and sildenafil (10 nmol/L), as indicated. **(C)** Cell surface area (3 independent experiments, ne54) and **(D)** percentage of NFAT-GFP nuclear translocation (4 independent experiments, n e76) calculated for untreated control, NRVMs treated for 48 hours with NE (10 μ mol/L) or myrPKI alone (10 μ mol/L), or in combination with NE, or NE and BAY 60-7550 (10 μ mol/L), NE and sildenafil (10 nmol/L) as indicated. **(E-F)** NFAT-GFP nuclear translocation measurements (3 independent experiments) for untreated control, NE (10 μ mol/L)-treated NRVMs or NRVMs treated with NE (10 μ mol/L) and transfected either with siPDE2 or with the control oligo siGLO Red in the presence or absence of DT-2 (10 μ mol/L) or of myrPKI (10 μ mol/L). **(G)** [³H] leucine incorporation assay performed in NRVMs treated with NE in combination with BAY 60-7550 (10 μ mol/L) and the PKA inhibitors H89 or cAMPS-Rp (n e 4 independent experiments). **(H)** NFAT-GFP nuclear translocation measurements (2 independent experiments) for untreated control, NRVMs transfected with Ht31 and treated with NE and BAY 60-7550. All data represent mean \pm s.e.m. One-way ANOVA and Tukey's multiple comparison tests were utilised. Pixel size = 0.1075 μ m. * p < 0.05, ** p < 0.01, *** p < 0.005.



1

2 **Figure 5. PDE2 modulates a local pool of cAMP with anti-hypertrophic effects.**

3 NRVM were transfected with catalytically inactive PDE4D3 (panels **A, B**), catalytically inactive
4 PDE3A2 (panels **C, D**) or catalytically inactive PDE2A (panels **E, F**) and cells surface area was
5 measured in the absence or presence of 10 $\mu\text{mol/L}$ NE for 48 hrs. In each panel, the cell surface
6 area is shown as mean \pm s.e.m on the left and on the right an overlay of DIC and fluorescence
7 images showing one NRVM overexpressing the catalytically inactive PDE and in the same field a
8 non-transfected control cardiomyocyte is presented. For all conditions ne25 cells from three
9 independent experiments. Pixel size = 0.1075 μm . Scale bar: 10 μm . For all experiments *t*-test
10 statistical analysis was performed. *** $p < 0.005$; ns= not significant.

11

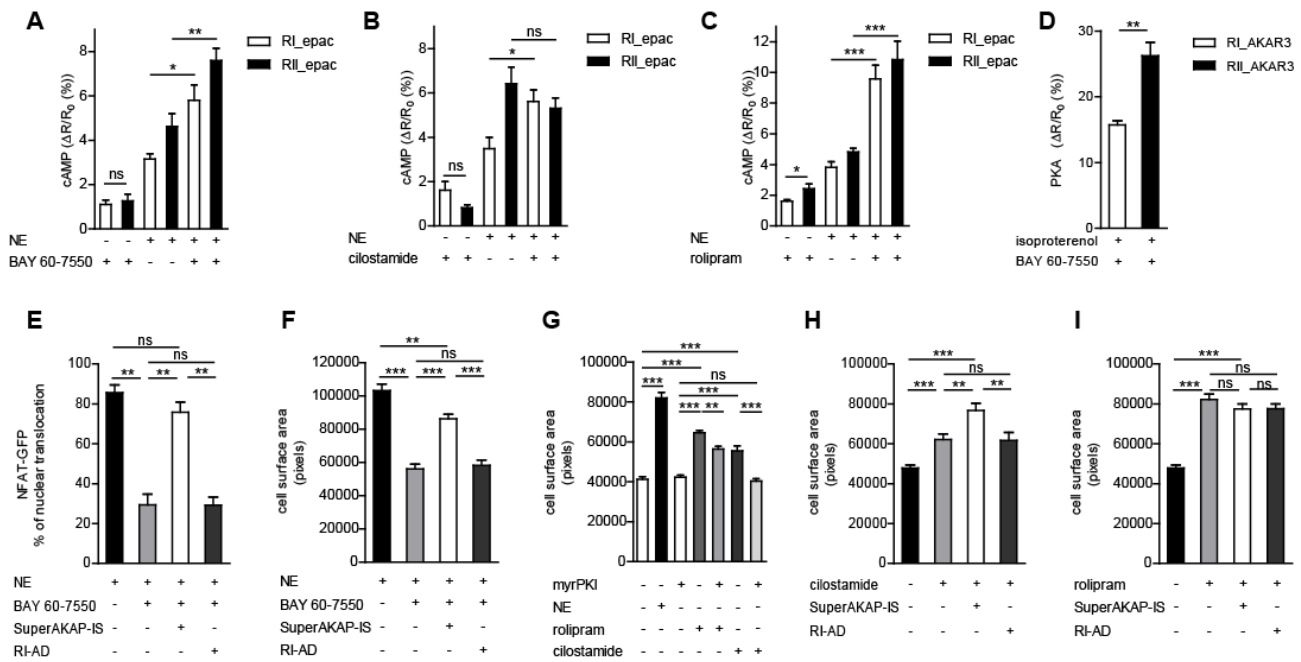


Figure 6. PKAII mediates the anti-hypertrophic effects of BAY 60-7550.

Quantification of cAMP changes induced by BAY 60-7550 (10 μ mol/L), NE (10nmol/L), NE plus BAY 60-7550 (**A**) or by cilostamide (10 μ mol/L), NE (10nmol/L), or NE plus cilostamide (**B**), or by rolipram (10 μ mol/L), NE (10nmol/L), or NE plus rolipram (**C**) in NRVMs expressing either RI-epac or RII-epac. ne4. (**D**) Quantification of PKA isoform-selective activation induced by isoproterenol (10nmol/L) and BAY 60-7550 measured in NRVMs expressing the FRET sensors RI_AKAR3 or RII_AKAR3¹⁶. ne3. (**E**) Percentage of cells showing nuclear translocation of NFAT-GFP (**F**) and cell size measured for NE-treated or NE+BAY 60-7550 treated NRVMs untransfected or transfected with either SuperAKAP-IS or RI-AD. ne4. (**G**) Cell surface area measurements of NRVMs treated for 48 hours as indicated. Cell size measured untransfected NRVMs or NRVMs transfected with either SuperAKAP-IS or RI-AD and treated with cilostamide (**H**) or rolipram (**I**) as indicated; ne34. All data represent mean \pm s.e.m. For experiments in A-D a t-test statistical analysis was performed. In E-I, one-way ANOVA and Tukey's multiple comparison tests were utilised. *** p < 0.005; ** p < 0.01; * p < 0.05; ns= not significant.

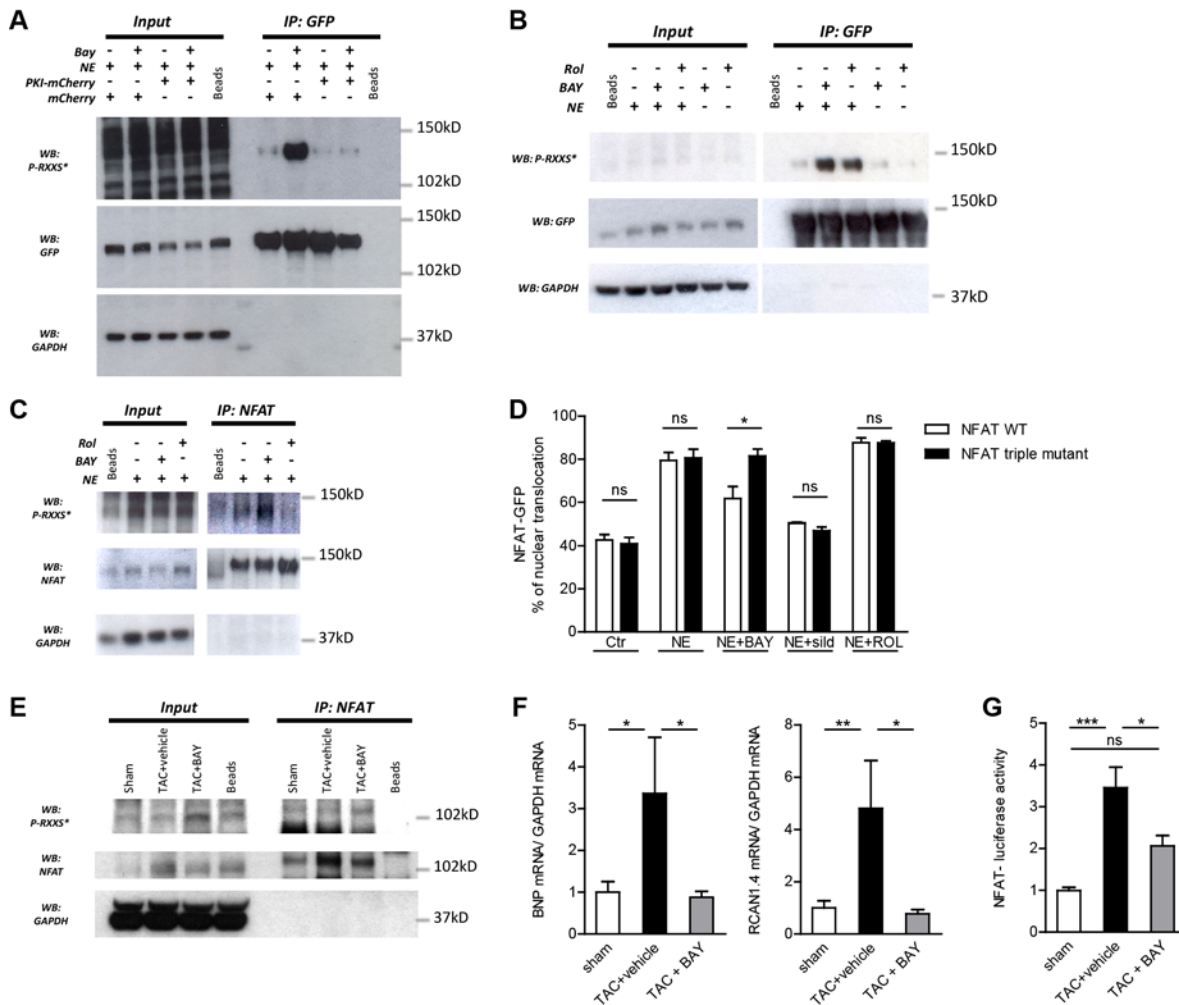


Figure 7. The anti-hypertrophic effect of PDE2 inhibition requires PKA-mediated phosphorylation of NFAT.

(A) Representative GFP-pull down experiment from lysate of NRVMs expressing NFAT-GFP, PKI-mcherry or mcherry. Cells were treated with NE (10 μ mol/L) and BAY 60-7550 (10 μ mol/L) as indicated. Blots were probed with anti Phospho-PKA substrate, anti GFP and anti GAPDH antibodies. n = 3. (B) Representative GFP-pull down experiment from lysate of NRVMs expressing NFAT-GFP and treated with NE (10 μ mol/L), BAY 60-7550 (10 μ mol/L) and Rolipram (10 μ mol/L) as indicated. Blots were probed with anti Phospho-PKA substrate, anti GFP and anti GAPDH antibodies. n = 3. (C) Representative immunoprecipitation of endogenous NFAT performed on lysates from NRVMs treated with NE, BAY 60-7550 and rolipram as indicated. Blots were probed with anti Phospho-PKA substrate, anti NFAT and anti GAPDH antibodies. n = 3. (D) Nuclear translocation of NFAT-GFP wild type or NFAT-GFP triple mutant (S245A/S269A/S294A) calculated for untreated NRVMs, NRVMs treated for 48 hours with NE (10 μ mol/L), NE and BAY 60-7550 (10 μ mol/L), NE and sildenafil (10 nmol/L), or NE and rolipram (10 μ mol/L); n=3 independent experiments. (E) Representative immunoprecipitation of endogenous NFAT performed on mouse left ventricles whole cell lysates from sham, TAC+vehicle or TAC+BAY 60-7550 mice as indicated. Blots were probed with anti Phospho-PKA substrate, anti NFAT and anti GAPDH antibodies. Representative of 4 independent experiments (F) BNP (left) and RCAN1.4 (right) mRNA levels measured in LV samples from sham, TAC+vehicle or TAC+BAY 60-7550 mice as indicated (n=3-7). (G) Quantification of NFAT luciferase activity in LV homogenates from TAC mice after two weeks treatment with BAY 60-7550, normalized to sham values. Four repeats per sample was performed. All data represent mean \pm s.e.m. In D *t*-test was utilised, one-way ANOVA and Tukey's multiple comparison tests were performed in F and G. Pixel size= 0.1075 μ m. * p < 0.05; ** p < 0.01; ns= not significant.

References

1. El-Armouche A and Eschenhagen T. Beta-adrenergic stimulation and myocardial function in the failing heart. *Heart Fail Rev.* 2009;14:225-41.
2. Zaccolo M and Pozzan T. Discrete microdomains with high concentration of cAMP in stimulated rat neonatal cardiac myocytes. *Science.* 2002;295:1711-5.
3. Nikolaev VO, Moshkov A, Lyon AR, Miragoli M, Novak P, Paur H, Lohse MJ, Korchev YE, Harding SE and Gorelik J. Beta2-adrenergic receptor redistribution in heart failure changes cAMP compartmentation. *Science.* 2010;327:1653-7.
4. Hayes JS, Brunton LL, Brown JH, Reese JB and Mayer SE. Hormonally specific expression of cardiac protein kinase activity. *Proceedings of the National Academy of Sciences of the United States of America.* 1979;76:1570-4.
5. Hayes JS and Brunton LL. Functional compartments in cyclic nucleotide action. *J Cyclic Nucleotide Res.* 1982;8:1-16.
6. Di Benedetto G, Zoccarato A, Lissandron V, Terrin A, Li X, Houslay MD, Baillie GS and Zaccolo M. Protein kinase A type I and type II define distinct intracellular signaling compartments. *Circ Res.* 2008;103:836-44.
7. Scott JD and Santana LF. A-kinase anchoring proteins: getting to the heart of the matter. *Circulation.* 2010;121:1264-71.
8. Carr DW, Stofko-Hahn RE, Fraser ID, Bishop SM, Acott TS, Brennan RG and Scott JD. Interaction of the regulatory subunit (RII) of cAMP-dependent protein kinase with RII-anchoring proteins occurs through an amphipathic helix binding motif. *The Journal of biological chemistry.* 1991;266:14188-92.
9. Hulme JT, Westenbroek RE, Scheuer T and Catterall WA. Phosphorylation of serine 1928 in the distal C-terminal domain of cardiac CaV1.2 channels during beta1-adrenergic regulation. *Proc Natl Acad Sci U S A.* 2006;103:16574-9.
10. Lygren B, Carlson CR, Santamaria K, Lissandron V, McSorley T, Litzenberg J, Lorenz D, Wiesner B, Rosenthal W, Zaccolo M, Tasken K and Klussmann E. AKAP complex regulates Ca²⁺ re-uptake into heart sarcoplasmic reticulum. *EMBO Rep.* 2007;8:1061-7.
11. Marx SO, Kurokawa J, Reiken S, Motoike H, D'Armiento J, Marks AR and Kass RS. Requirement of a macromolecular signaling complex for beta adrenergic receptor modulation of the KCNQ1-KCNE1 potassium channel. *Science.* 2002;295:496-9.
12. Gold MG, Lygren B, Dokurno P, Hoshi N, McConnachie G, Tasken K, Carlson CR, Scott JD and Barford D. Molecular basis of AKAP specificity for PKA regulatory subunits. *Molecular cell.* 2006;24:383-95.
13. Banky P, Newlon MG, Roy M, Garrod S, Taylor SS and Jennings PA. Isoform-specific differences between the type Ialpha and IIalpha cyclic AMP-dependent protein kinase anchoring domains revealed by solution NMR. *The Journal of biological chemistry.* 2000;275:35146-52.
14. Maurice DH, Ke H, Ahmad F, Wang Y, Chung J and Manganiello VC. Advances in targeting cyclic nucleotide phosphodiesterases. *Nature reviews Drug discovery.* 2014;13:290-314.
15. Leroy J, Abi-Gerges A, Nikolaev VO, Richter W, Lechene P, Mazet JL, Conti M, Fischmeister R and Vandecasteele G. Spatiotemporal dynamics of beta-adrenergic cAMP signals and L-type Ca²⁺ channel regulation in adult rat ventricular myocytes: role of phosphodiesterases. *Circ Res.* 2008;102:1091-100.
16. Stangherlin A, Gesellchen F, Zoccarato A, Terrin A, Fields LA, Berrera M, Surdo NC, Craig MA, Smith G, Hamilton G and Zaccolo M. cGMP signals modulate cAMP levels in a compartment-specific manner to regulate catecholamine-dependent signaling in cardiac myocytes. *Circulation research.* 2011;108:929-39.
17. Mongillo M, McSorley T, Evellin S, Sood A, Lissandron V, Terrin A, Huston E, Hannawacker A, Lohse MJ, Pozzan T, Houslay MD and Zaccolo M. Fluorescence resonance energy transfer-based analysis of cAMP dynamics in live neonatal rat cardiac myocytes reveals distinct functions of compartmentalized phosphodiesterases. *Circulation research.* 2004;95:67-75.
18. Mongillo M, Tocchetti CG, Terrin A, Lissandron V, Cheung YF, Dostmann WR, Pozzan T, Kass DA, Paolocci N, Houslay MD and Zaccolo M. Compartmentalized phosphodiesterase-2 activity blunts beta-adrenergic cardiac inotropy via an NO/cGMP-dependent pathway. *Circulation research.* 2006;98:226-34.

- 1 19. Haworth RS, Cuello F and Avkiran M. Regulation by phosphodiesterase isoforms of protein kinase A-
2 mediated attenuation of myocardial protein kinase D activation. *Basic research in cardiology*. 2011;106:51-
3 63.
- 4 20. Nichols CB, Chang CW, Ferrero M, Wood BM, Stein ML, Ferguson AJ, Ha D, Rigor RR, Bossuyt S and
5 Bossuyt J. beta-adrenergic signaling inhibits Gq-dependent protein kinase D activation by preventing
6 protein kinase D translocation. *Circulation research*. 2014;114:1398-409.
- 7 21. Mudd JO and Kass DA. Tackling heart failure in the twenty-first century. *Nature*. 2008;451:919-28.
- 8 22. White DC, Hata JA, Shah AS, Glower DD, Lefkowitz RJ and Koch WJ. Preservation of myocardial
9 beta-adrenergic receptor signaling delays the development of heart failure after myocardial infarction. *Proc*
10 *Natl Acad Sci U S A*. 2000;97:5428-33.
- 11 23. Lai NC, Roth DM, Gao MH, Fine S, Head BP, Zhu J, McKirnan MD, Kwong C, Dalton N, Urasawa K,
12 Roth DA and Hammond HK. Intracoronary delivery of adenovirus encoding adenylyl cyclase VI increases left
13 ventricular function and cAMP-generating capacity. *Circulation*. 2000;102:2396-401.
- 14 24. Sucharov CC, Dockstader K, Nunley K, McKinsey TA and Bristow M. beta-Adrenergic receptor
15 stimulation and activation of protein kinase A protect against alpha1-adrenergic-mediated phosphorylation
16 of protein kinase D and histone deacetylase 5. *Journal of cardiac failure*. 2011;17:592-600.
- 17 25. Simpson P. Stimulation of hypertrophy of cultured neonatal rat heart cells through an alpha 1-
18 adrenergic receptor and induction of beating through an alpha 1- and beta 1-adrenergic receptor
19 interaction. Evidence for independent regulation of growth and beating. *Circ Res*. 1985;56:884-94.
- 20 26. Martins TJ, Mumby MC and Beavo JA. Purification and characterization of a cyclic GMP-stimulated
21 cyclic nucleotide phosphodiesterase from bovine tissues. *The Journal of biological chemistry*.
22 1982;257:1973-9.
- 23 27. Nickl CK, Raidas SK, Zhao H, Sausbier M, Ruth P, Tegge W, Brayden JE and Dostmann WR. (D)-Amino
24 acid analogues of DT-2 as highly selective and superior inhibitors of cGMP-dependent protein kinase Ialpha.
25 *Biochim Biophys Acta*. 2010;1804:524-32.
- 26 28. Takimoto E, Champion HC, Li M, Belardi D, Ren S, Rodriguez ER, Bedja D, Gabrielson KL, Wang Y and
27 Kass DA. Chronic inhibition of cyclic GMP phosphodiesterase 5A prevents and reverses cardiac hypertrophy.
28 *Nat Med*. 2005;11:214-22.
- 29 29. Hodges RR, Zoukhri D, Sergheraert C, Zieske JD and Dartt DA. Identification of vasoactive intestinal
30 peptide receptor subtypes in the lacrimal gland and their signal-transducing components. *Invest*
31 *Ophthalmol Vis Sci*. 1997;38:610-9.
- 32 30. Carr DW, Hausken ZE, Fraser ID, Stofko-Hahn RE and Scott JD. Association of the type II cAMP-
33 dependent protein kinase with a human thyroid RII-anchoring protein. Cloning and characterization of the
34 RII-binding domain. *The Journal of biological chemistry*. 1992;267:13376-82.
- 35 31. McCahill A, McSorley T, Huston E, Hill EV, Lynch MJ, Gall I, Keryer G, Lygren B, Tasken K, van Heeke
36 G and Houslay MD. In resting COS1 cells a dominant negative approach shows that specific, anchored PDE4
37 cAMP phosphodiesterase isoforms gate the activation, by basal cyclic AMP production, of AKAP-tethered
38 protein kinase A type II located in the centrosomal region. *Cellular signalling*. 2005;17:1158-73.
- 39 32. Terrin A, Monterisi S, Stangherlin A, Zoccarato A, Koschinski A, Surdo NC, Mongillo M, Sawa A,
40 Jordanides NE, Mountford JC and Zaccolo M. PKA and PDE4D3 anchoring to AKAP9 provides distinct
41 regulation of cAMP signals at the centrosome. *The Journal of cell biology*. 2012;198:607-21.
- 42 33. Carlson CR, Lygren B, Berge T, Hoshi N, Wong W, Tasken K and Scott JD. Delineation of type I
43 protein kinase A-selective signaling events using an RI anchoring disruptor. *The Journal of biological*
44 *chemistry*. 2006;281:21535-45.
- 45 34. Molkenkint JD, Lu JR, Antos CL, Markham B, Richardson J, Robbins J, Grant SR and Olson EN. A
46 calcineurin-dependent transcriptional pathway for cardiac hypertrophy. *Cell*. 1998;93:215-28.
- 47 35. Beals CR, Sheridan CM, Turck CW, Gardner P and Crabtree GR. Nuclear export of NF-ATc enhanced
48 by glycogen synthase kinase-3. *Science*. 1997;275:1930-4.
- 49 36. Sheridan CM, Heist EK, Beals CR, Crabtree GR and Gardner P. Protein kinase A negatively modulates
50 the nuclear accumulation of NF-ATc1 by priming for subsequent phosphorylation by glycogen synthase
51 kinase-3. *The Journal of biological chemistry*. 2002;277:48664-76.

- 1 37. Vega RB, Rothermel BA, Weinheimer CJ, Kovacs A, Naseem RH, Bassel-Duby R, Williams RS and
2 Olson EN. Dual roles of modulatory calcineurin-interacting protein 1 in cardiac hypertrophy. *Proceedings of*
3 *the National Academy of Sciences of the United States of America*. 2003;100:669-74.
- 4 38. Wilkins BJ, Dai YS, Bueno OF, Parsons SA, Xu J, Plank DM, Jones F, Kimball TR and Molkentin JD.
5 Calcineurin/NFAT coupling participates in pathological, but not physiological, cardiac hypertrophy.
6 *Circulation research*. 2004;94:110-8.
- 7 39. Asakura M, Kitakaze M, Takashima S, Liao Y, Ishikura F, Yoshinaka T, Ohmoto H, Node K, Yoshino K,
8 Ishiguro H, Asanuma H, Sanada S, Matsumura Y, Takeda H, Beppu S, Tada M, Hori M and Higashiyama S.
9 Cardiac hypertrophy is inhibited by antagonism of ADAM12 processing of HB-EGF: metalloproteinase
10 inhibitors as a new therapy. *Nature medicine*. 2002;8:35-40.
- 11 40. Zhang X, Szeto C, Gao E, Tang M, Jin J, Fu Q, Makarewich C, Ai X, Li Y, Tang A, Wang J, Gao H, Wang
12 F, Ge XJ, Kunapuli SP, Zhou L, Zeng C, Xiang KY and Chen X. Cardiotoxic and cardioprotective features of
13 chronic beta-adrenergic signaling. *Circulation research*. 2013;112:498-509.
- 14 41. Enns LC, Bible KL, Emond MJ and Ladiges WC. Mice lacking the Cbeta subunit of PKA are resistant to
15 angiotensin II-induced cardiac hypertrophy and dysfunction. *BMC research notes*. 2010;3:307.
- 16 42. Ha CH, Kim JY, Zhao J, Wang W, Jhun BS, Wong C and Jin ZG. PKA phosphorylates histone
17 deacetylase 5 and prevents its nuclear export, leading to the inhibition of gene transcription and
18 cardiomyocyte hypertrophy. *Proc Natl Acad Sci U S A*. 2010;107:15467-72.
- 19 43. Abrenica B, AlShaaban M and Czubryt MP. The A-kinase anchor protein AKAP121 is a negative
20 regulator of cardiomyocyte hypertrophy. *Journal of molecular and cellular cardiology*. 2009;46:674-81.
- 21 44. Nichols CB, Rossow CF, Navedo MF, Westenbroek RE, Catterall WA, Santana LF and McKnight GS.
22 Sympathetic stimulation of adult cardiomyocytes requires association of AKAP5 with a subpopulation of L-
23 type calcium channels. *Circ Res*. 2010;107:747-56.
- 24 45. Li J, Negro A, Lopez J, Bauman AL, Henson E, Dodge-Kafka K and Kapiloff MS. The mAKAPbeta
25 scaffold regulates cardiac myocyte hypertrophy via recruitment of activated calcineurin. *Journal of*
26 *molecular and cellular cardiology*. 2010;48:387-94.
- 27 46. Makarewich CA, Correll RN, Gao H, Zhang H, Yang B, Berretta RM, Rizzo V, Molkentin JD and Houser
28 SR. A caveolae-targeted L-type Ca(2)+ channel antagonist inhibits hypertrophic signaling without reducing
29 cardiac contractility. *Circ Res*. 2012;110:669-74.
- 30 47. Rinne A, Kapur N, Molkentin JD, Pogwizd SM, Bers DM, Banach K and Blatter LA. Isoform- and
31 tissue-specific regulation of the Ca(2+)-sensitive transcription factor NFAT in cardiac myocytes and heart
32 failure. *American journal of physiology Heart and circulatory physiology*. 2010;298:H2001-9.
- 33 48. Mehel H, Emons J, Vettel C, Wittkopper K, Seppelt D, Dewenter M, Lutz S, Sossalla S, Maier LS,
34 Lechene P, Leroy J, Lefebvre F, Varin A, Eschenhagen T, Nattel S, Dobrev D, Zimmermann WH, Nikolaev VO,
35 Vandecasteele G, Fischmeister R and El-Armouche A. Phosphodiesterase-2 is Upregulated in Human Failing
36 Hearts and Blunts beta-Adrenergic Responses in Cardiomyocytes. *Journal of the American College of*
37 *Cardiology*. 2013.
- 38 49. Hua R, Adamczyk A, Robbins C, Ray G and Rose RA. Distinct patterns of constitutive
39 phosphodiesterase activity in mouse sinoatrial node and atrial myocardium. *PloS one*. 2012;7:e47652.
- 40 50. Aye TT, Soni S, van Veen TA, van der Heyden MA, Cappadona S, Varro A, de Weger RA, de Jonge N,
41 Vos MA, Heck AJ and Scholten A. Reorganized PKA-AKAP associations in the failing human heart. *Journal of*
42 *molecular and cellular cardiology*. 2011.
- 43 51. Perrino C, Naga Prasad SV, Mao L, Noma T, Yan Z, Kim HS, Smithies O and Rockman HA.
44 Intermittent pressure overload triggers hypertrophy-independent cardiac dysfunction and vascular
45 rarefaction. *J Clin Invest*. 2006;116:1547-60.
- 46 52. Frey N, Katus HA, Olson EN and Hill JA. Hypertrophy of the heart: a new therapeutic target?
47 *Circulation*. 2004;109:1580-9.
- 48 53. Esposito G, Rapacciuolo A, Naga Prasad SV, Takaoka H, Thomas SA, Koch WJ and Rockman HA.
49 Genetic alterations that inhibit in vivo pressure-overload hypertrophy prevent cardiac dysfunction despite
50 increased wall stress. *Circulation*. 2002;105:85-92.
- 51 54. Koitabashi N and Kass DA. Reverse remodeling in heart failure--mechanisms and therapeutic
52 opportunities. *Nat Rev Cardiol*. 2011;9:147-57.

- 1 55. Bristow MR. Treatment of chronic heart failure with beta-adrenergic receptor antagonists: a
2 convergence of receptor pharmacology and clinical cardiology. *Circ Res*. 2011;109:1176-94.
- 3 56. Metra M, Eichhorn E, Abraham WT, Linseman J, Bohm M, Corbalan R, DeMets D, De Marco T,
4 Elkayam U, Gerber M, Komajda M, Liu P, Mareev V, Perrone SV, Poole-Wilson P, Roecker E, Stewart J,
5 Swedberg K, Tendera M, Wiens B and Bristow MR. Effects of low-dose oral enoximone administration on
6 mortality, morbidity, and exercise capacity in patients with advanced heart failure: the randomized, double-
7 blind, placebo-controlled, parallel group ESSENTIAL trials. *Eur Heart J*. 2009;30:3015-26.
- 8 57. Gesztelyi R, Zsuga J, Hajdu P, Szabo JZ, Cseppento A and Szentmiklosi AJ. Positive inotropic effect of
9 the inhibition of cyclic GMP-stimulated 3',5'-cyclic nucleotide phosphodiesterase (PDE2) on guinea pig left
10 atria in eu- and hyperthyroidism. *Gen Physiol Biophys*. 2003;22:501-13.

11